

(12) **United States Patent**
Lasseter et al.

(10) **Patent No.:** **US 7,715,950 B2**
(45) **Date of Patent:** **May 11, 2010**

(54) **NON-INVERTER BASED DISTRIBUTED ENERGY RESOURCE FOR USE IN A DYNAMIC DISTRIBUTION SYSTEM**

(75) Inventors: **Robert H. Lasseter**, Madison, WI (US);
Shashank Krishnamurthy, Rocky Hill, CT (US)

(73) Assignee: **Wisconsin Alumni Research Foundation**, Madison, WI (US)

(*) Notice: Subject to any disclaimer, the term of this patent is extended or adjusted under 35 U.S.C. 154(b) by 305 days.

(21) Appl. No.: **11/681,014**

(22) Filed: **Mar. 1, 2007**

(65) **Prior Publication Data**

US 2008/0215187 A1 Sep. 4, 2008

(51) **Int. Cl.**

G05D 11/00 (2006.01)
H02P 27/00 (2006.01)
G06F 19/00 (2006.01)
B60T 7/12 (2006.01)

(52) **U.S. Cl.** **700/287**; 318/798; 700/286;
700/290; 701/99; 701/103; 701/104

(58) **Field of Classification Search** 700/287,
700/286, 290; 701/99, 10; 318/798
See application file for complete search history.

(56) **References Cited**

U.S. PATENT DOCUMENTS

4,096,394 A	6/1978	Ullmann et al.
4,315,163 A	2/1982	Bienville
5,041,959 A	8/1991	Walker
5,198,698 A	3/1993	Paul et al.
5,329,222 A	7/1994	Gyugyi et al.
5,536,976 A	7/1996	Churchill
5,559,704 A	9/1996	Vanek et al.
5,563,802 A	10/1996	Plahn et al.

5,596,492 A	1/1997	Divan et al.
5,614,770 A	3/1997	Suelzle
5,710,699 A	1/1998	King et al.
5,745,356 A	4/1998	Tassinato et al.
5,811,960 A	9/1998	Van Sickle et al.

(Continued)

OTHER PUBLICATIONS

Son et al., "A Newton-Type Current Injection Model of UPFC for Studying Low Frequency Oscillations" IEEE p. 1 abstract.*

(Continued)

Primary Examiner—Thomas H Stevens

Assistant Examiner—Albert DeCady

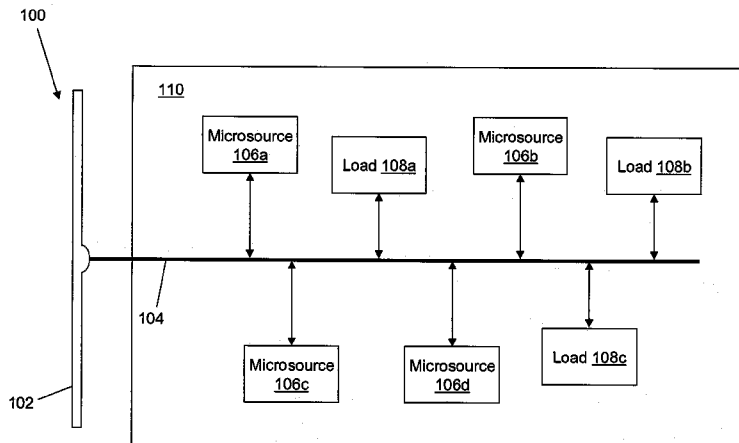
(74) *Attorney, Agent, or Firm*—Foley & Lardner LLP

(57)

ABSTRACT

A microsource is provided, which includes a generator, a prime mover, and a controller. The prime mover includes a shaft connected to drive the generator to generate power at a frequency controlled by a rotation rate of the shaft. The controller calculates an operating frequency for the generator based on a comparison between a power set point and a measured power flow. A requested shaft speed for the prime mover is calculated by combining a maximum frequency change, a minimum frequency change, and the calculated operating frequency. A shaft speed adjustment is calculated for the prime mover based on a comparison between the requested shaft speed and a measured shaft speed of the prime mover. A fuel command for the prime mover is calculated based on the shaft speed adjustment. A rotation rate of the shaft of the prime mover is adjusted based on the calculated fuel command to control the frequency.

20 Claims, 12 Drawing Sheets



U.S. PATENT DOCUMENTS

6,014,015 A 1/2000 Thorne et al.
 6,111,764 A 8/2000 Atou et al.
 6,134,124 A 10/2000 Jungreis et al.
 6,172,432 B1 1/2001 Schnackenberg et al.
 6,188,205 B1 2/2001 Tanimoto et al.
 6,219,591 B1 4/2001 Vu et al.
 6,219,623 B1 4/2001 Wills
 6,249,411 B1 6/2001 Hemena et al.
 6,252,310 B1 6/2001 Wilhelm
 6,285,917 B1 9/2001 Sekiguchi et al.
 6,288,456 B1 9/2001 Crafty
 6,347,027 B1 2/2002 Nelson et al.
 6,356,471 B1 3/2002 Fang
 6,359,423 B1 3/2002 Noro
 6,465,910 B2 10/2002 Young et al.
 6,693,809 B2 2/2004 Engler
 6,787,933 B2 9/2004 Claude et al.
 6,812,586 B2 11/2004 Wacknow et al.
 6,870,279 B2 3/2005 Gilbreth et al.
 7,042,110 B2 5/2006 Mikhail et al.
 7,069,673 B2 7/2006 Kagoshima et al.
 7,116,010 B2 * 10/2006 Lasseter et al. 307/45
 2003/0036806 A1 2/2003 Schienbein et al.

2004/0051387 A1 3/2004 Lasseter et al.
 2004/0080165 A1 4/2004 Geis et al.
 2006/0208574 A1 9/2006 Lasseter et al.

OTHER PUBLICATIONS

Lasseter, Robert, Kevin Tomsovic, and Paolo Piagi. "Scenarios for Distributed Technology Applications with Steady State and Dynamic Models of Loads and Micro-Sources," Consortium for Electric Reliability Technology Solutions. Apr. 14, 2000, p. 305-308.
 DOE News, The DER Weekly, vol. 2, No. 10, pp. 1-4. Mar. 9, 2001.
 Lasseter, Robert, et al. "White Paper on Integration of Distributed Energy Resources the CERTS MicroGrid Concept," Consortium for Electric Reliability Technology Solutions, pp. 1-27. Apr. 2002.
 Lasseter, Robert, "MicroGrids," IEEE, No. 0-7803-7322-7, pp. 305-308. Jul. 2002.
 PCT International Search Report and Written Opinion for PCT/US2008/054566 dated Jul. 11, 2008.
 PCT International Search Report and Written Opinion for PCT/US2008/054572 dated Jul. 11, 2008.
 PCT International Search Report and Written Opinion for PCT/US2008/054577 dated Jul. 11, 2008.
 Office Action issued in USSN 11/681,024 mailed on May 27, 2009.

* cited by examiner

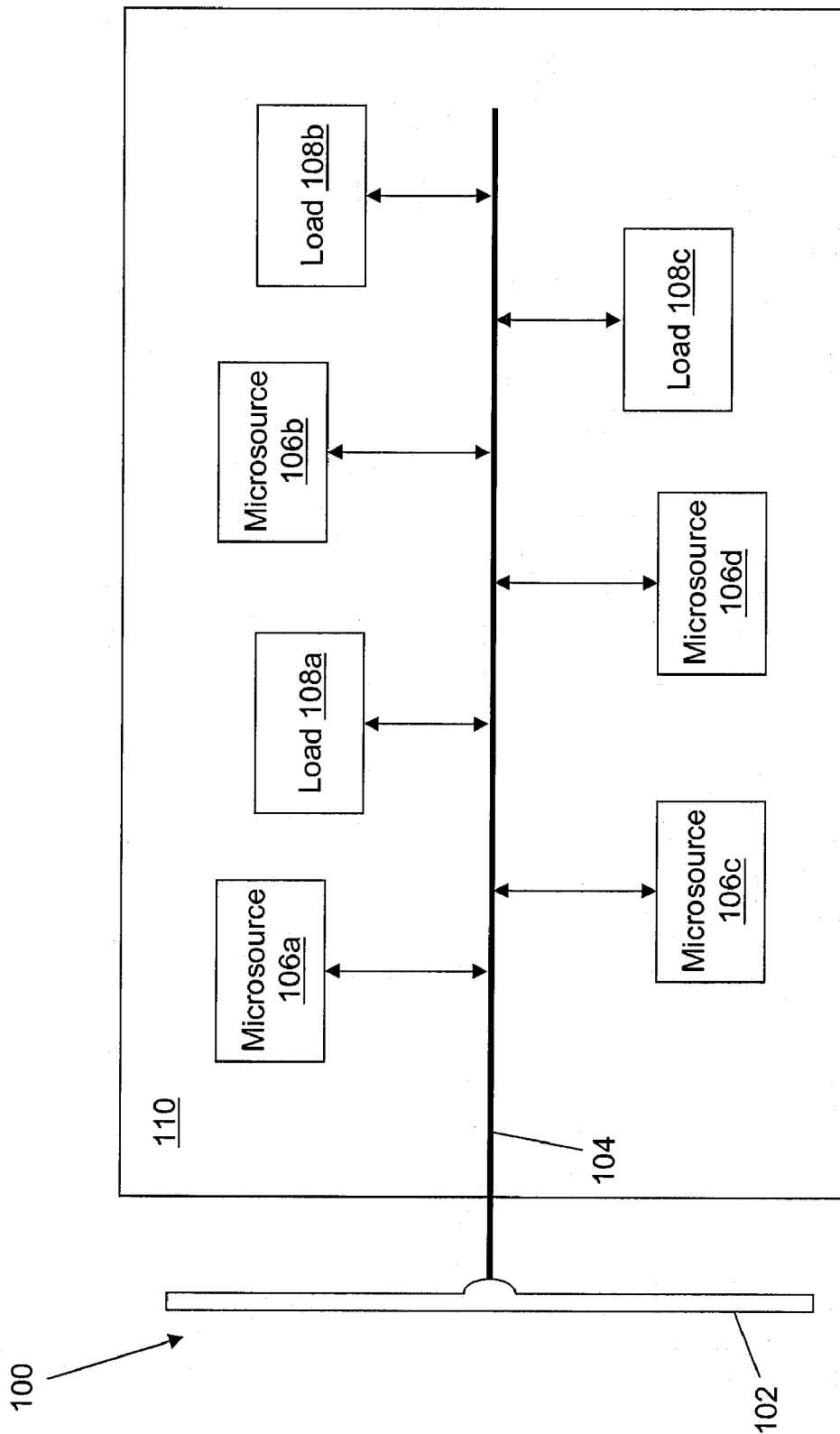
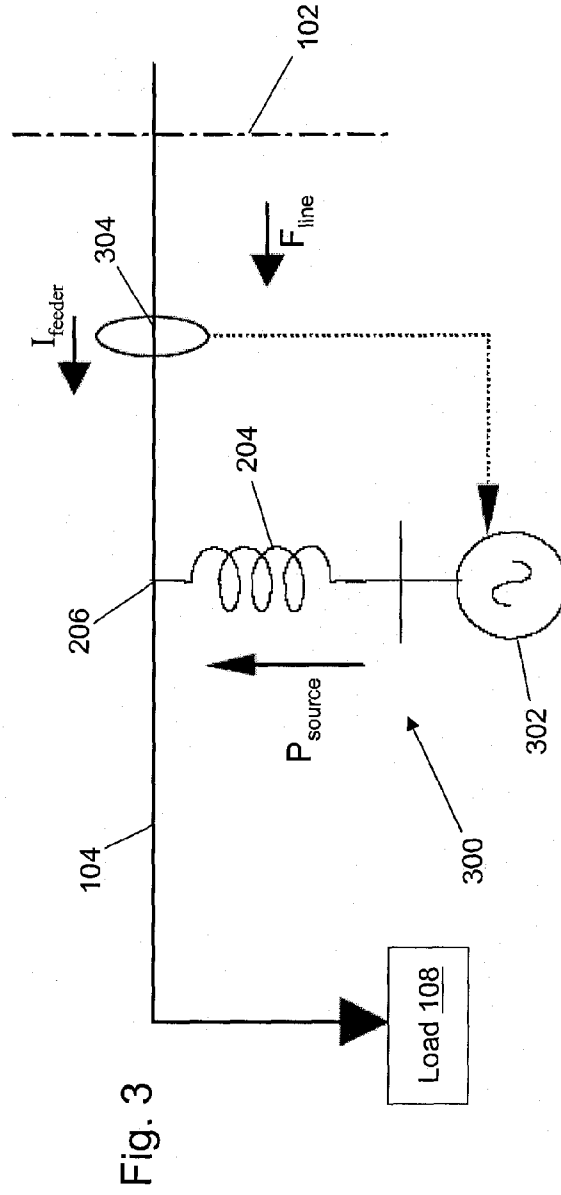
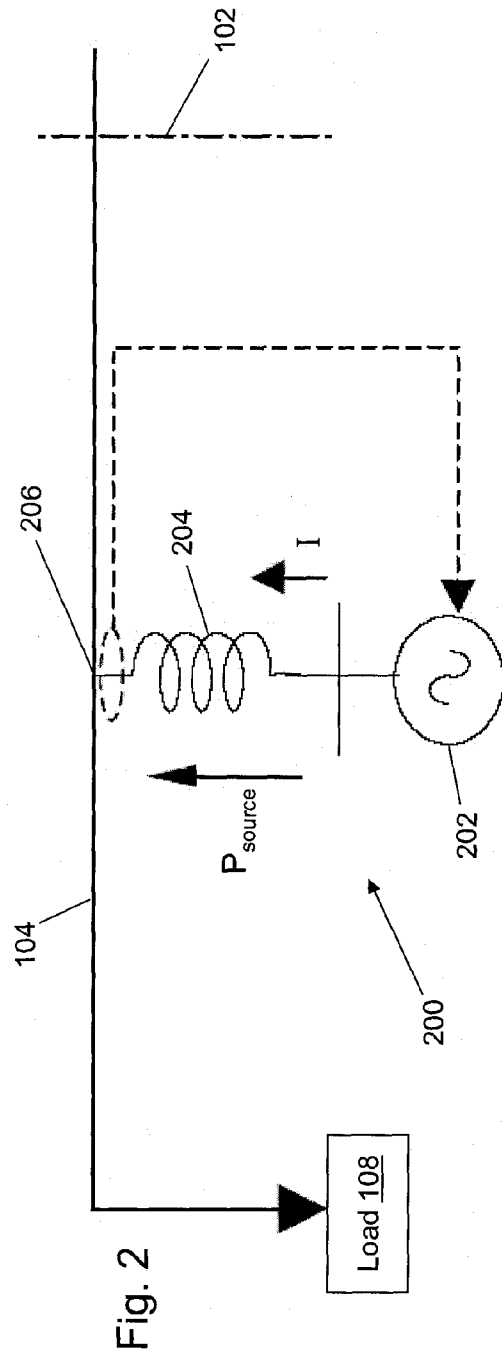


Fig. 1



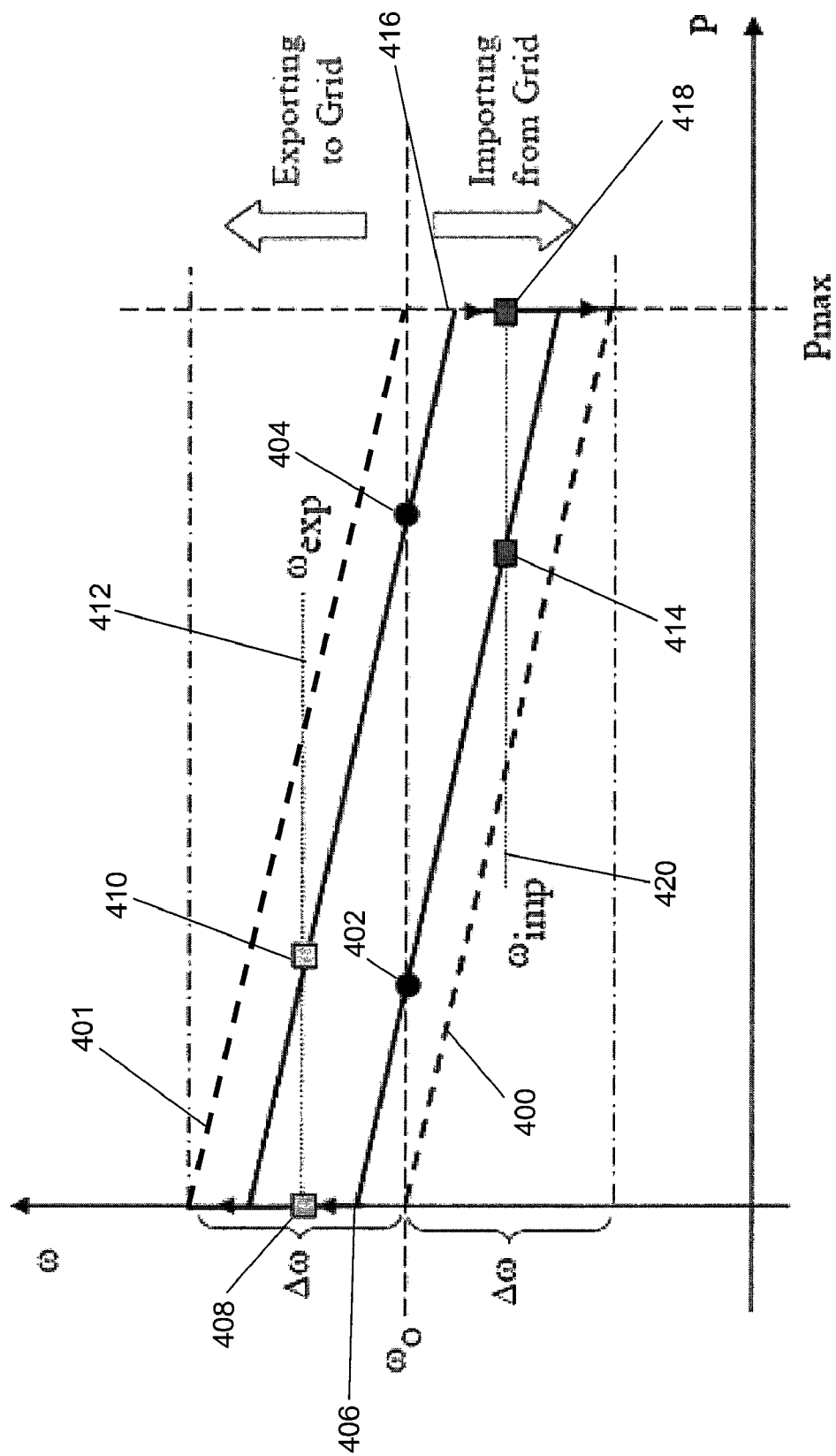


Fig. 4

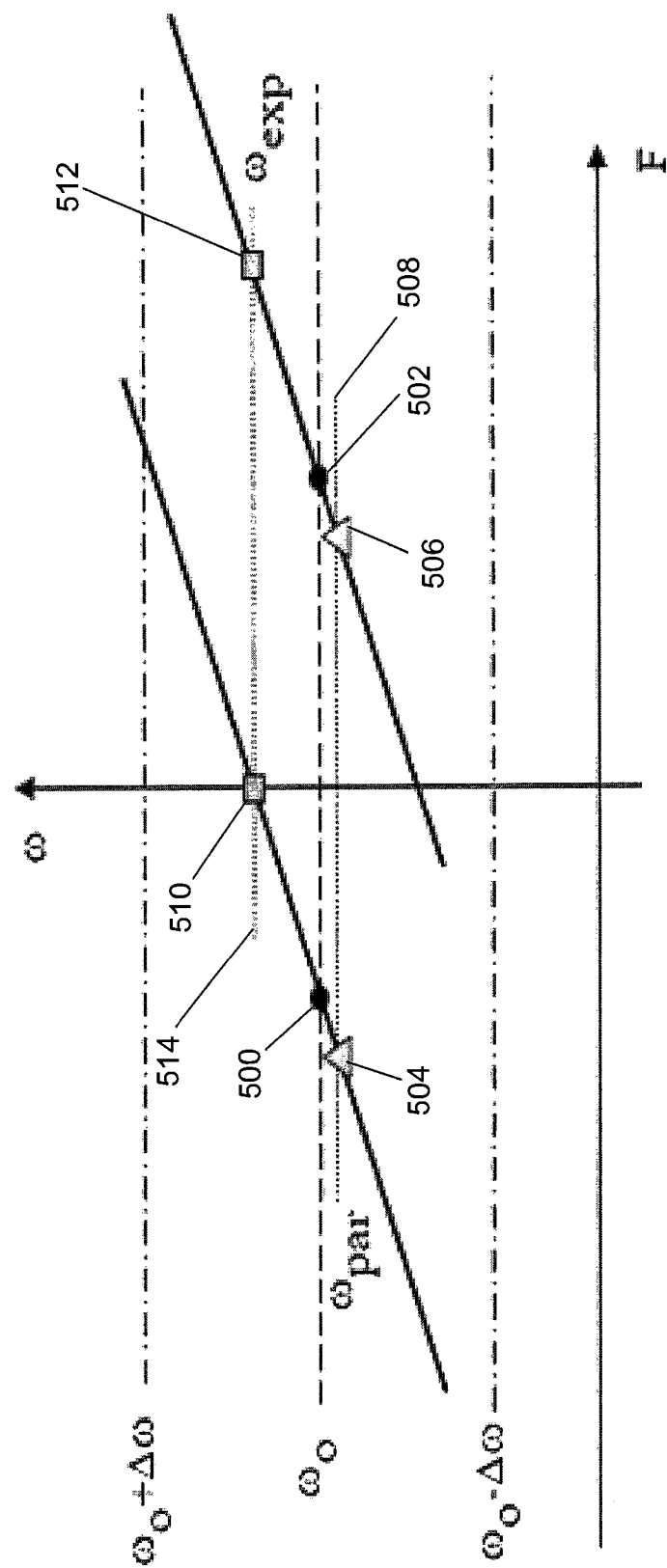
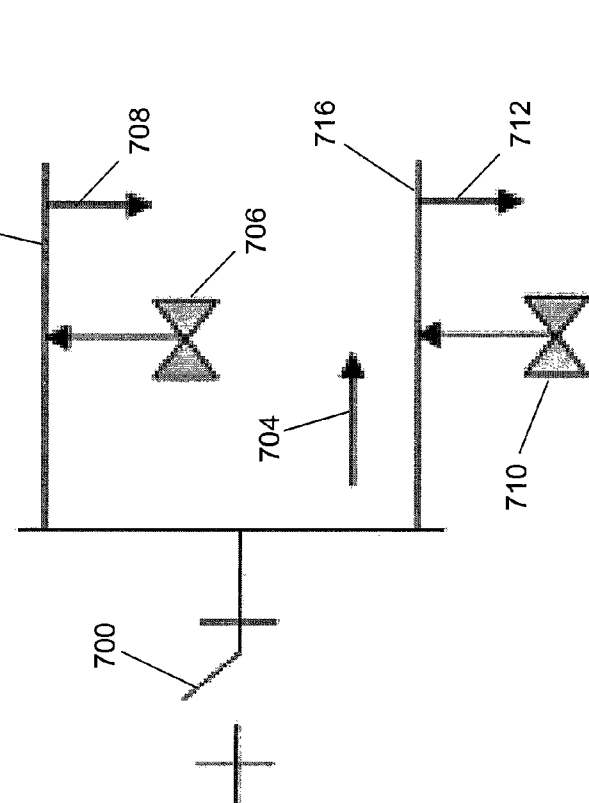
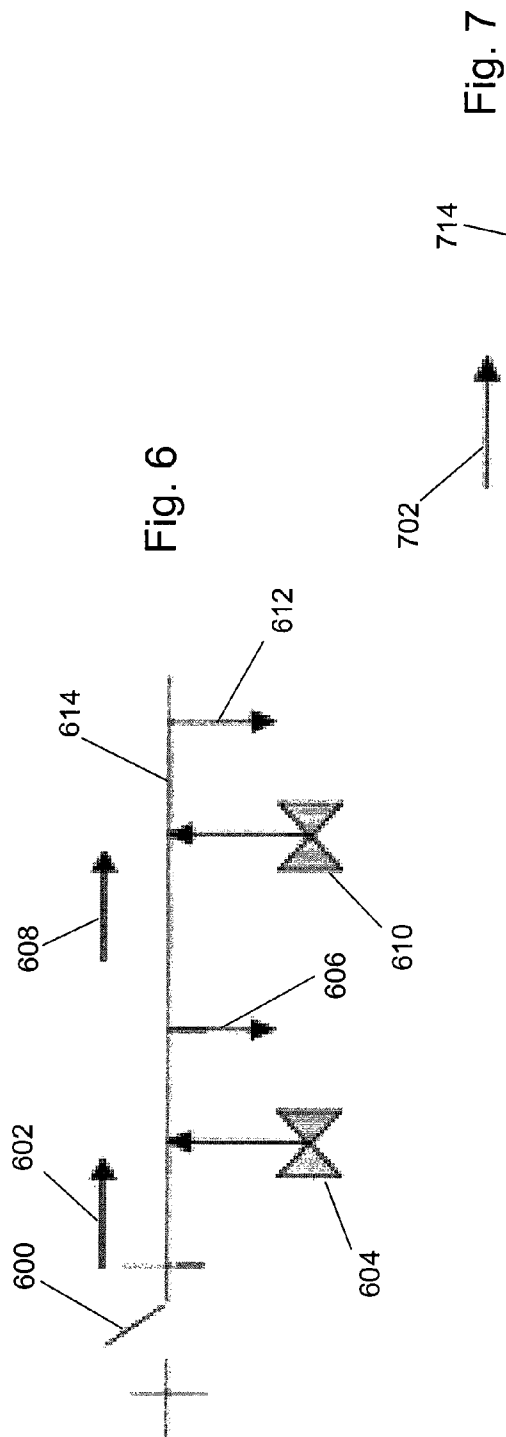


Fig. 5



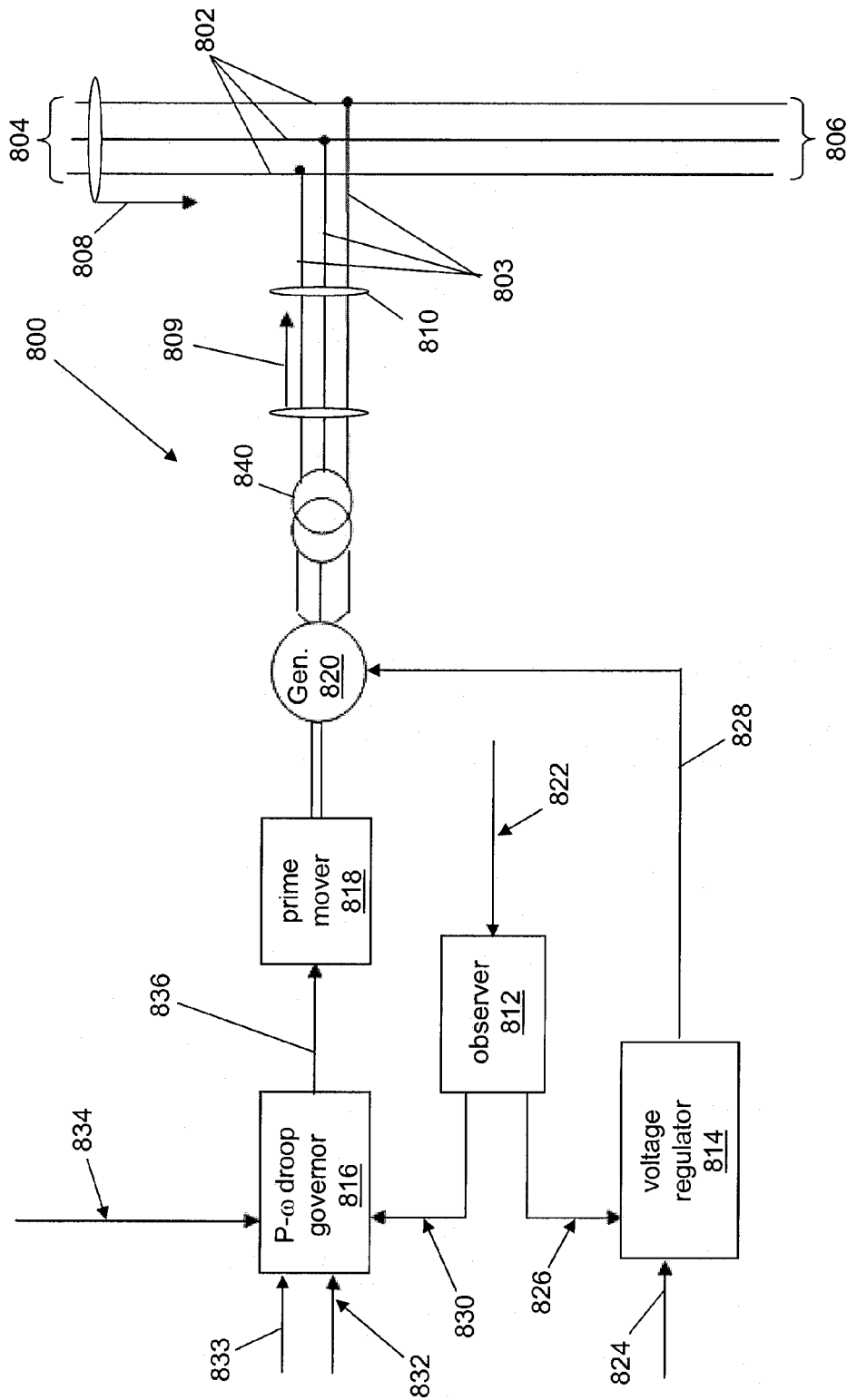


Fig. 8

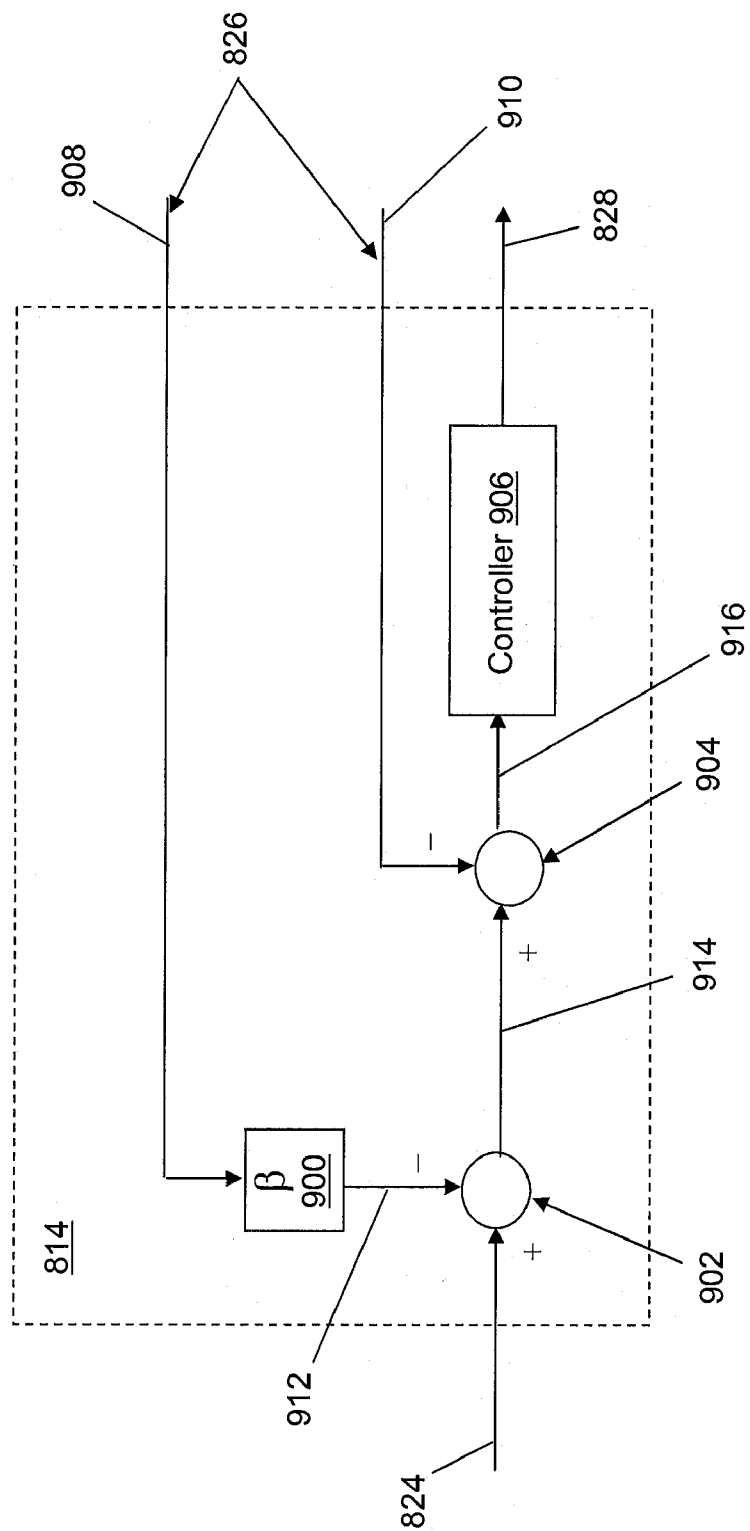


Fig. 9

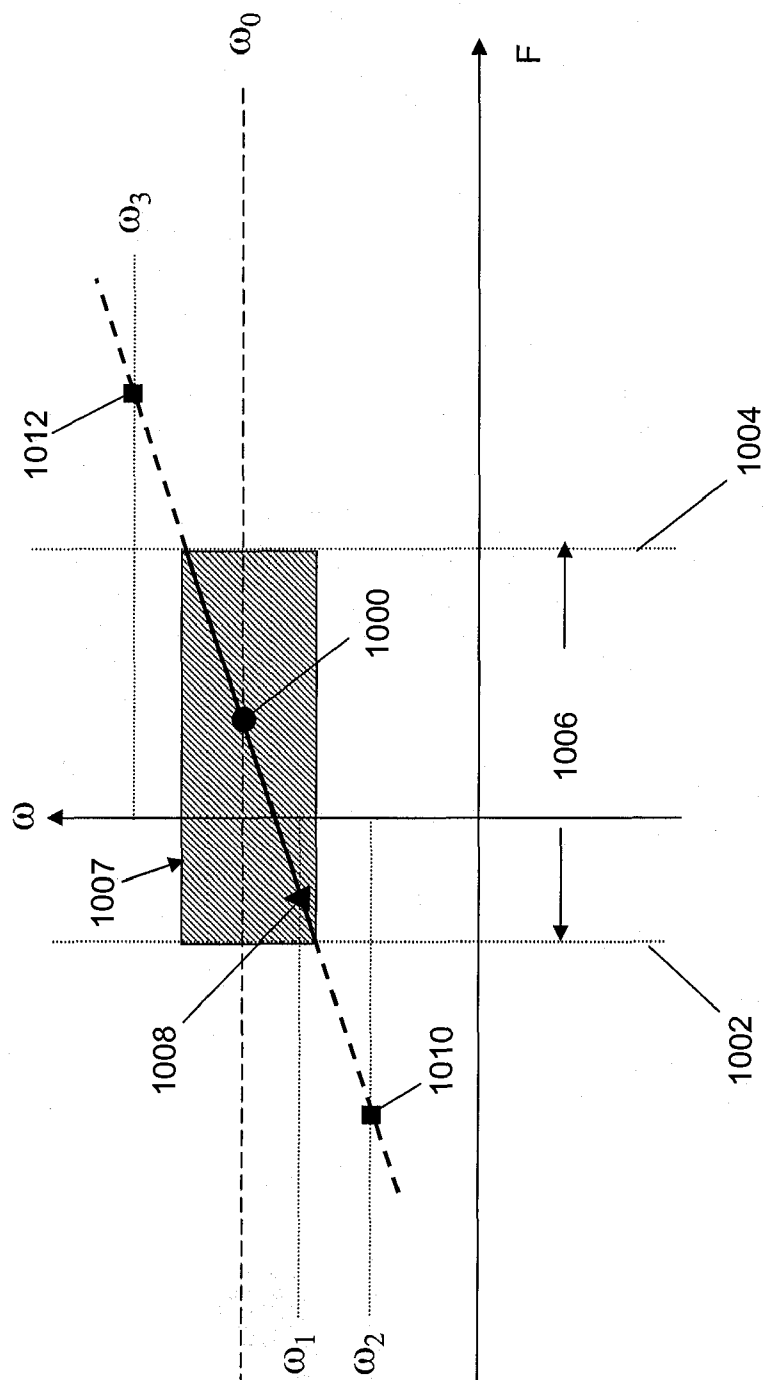


Fig. 10

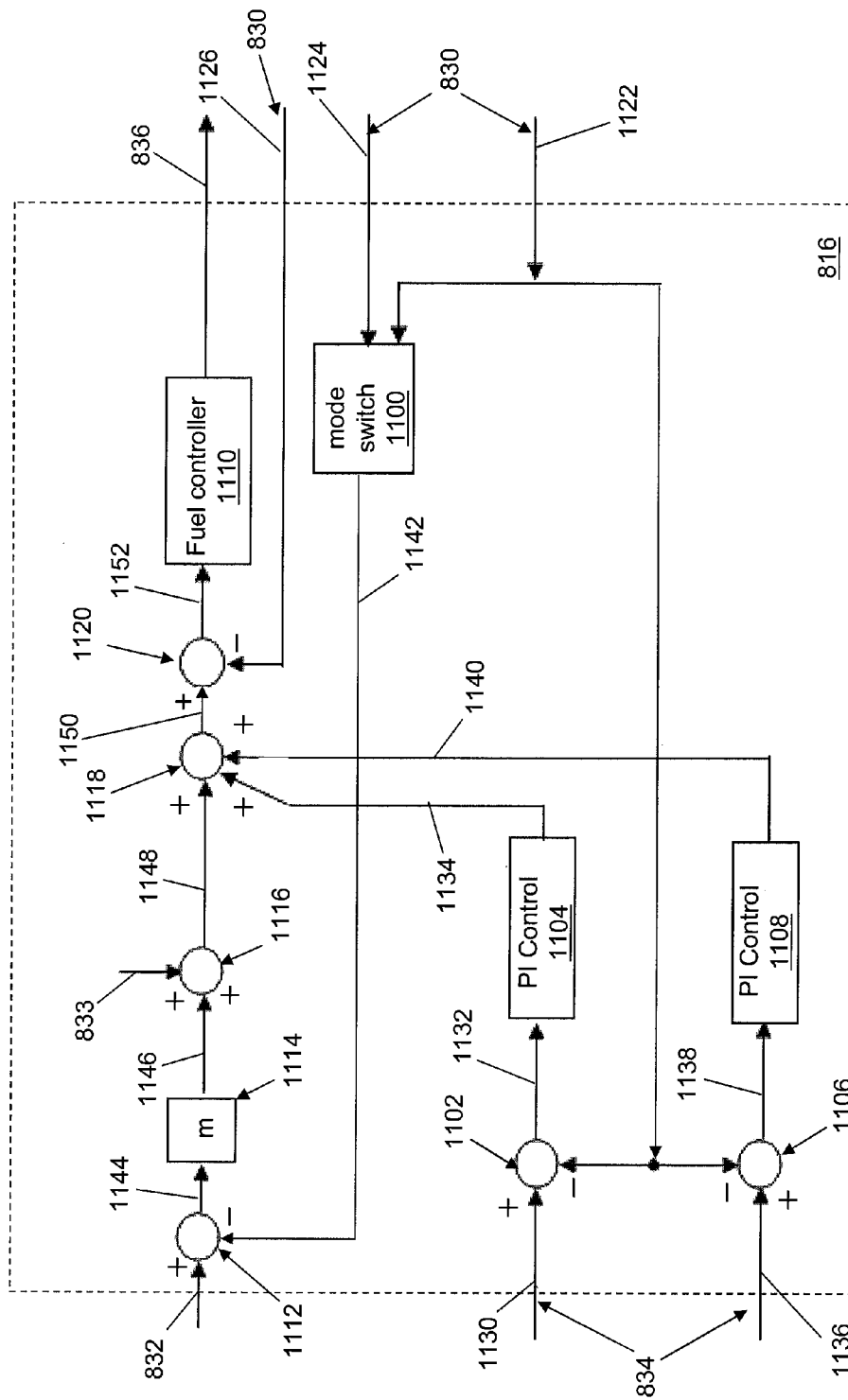


Fig. 11

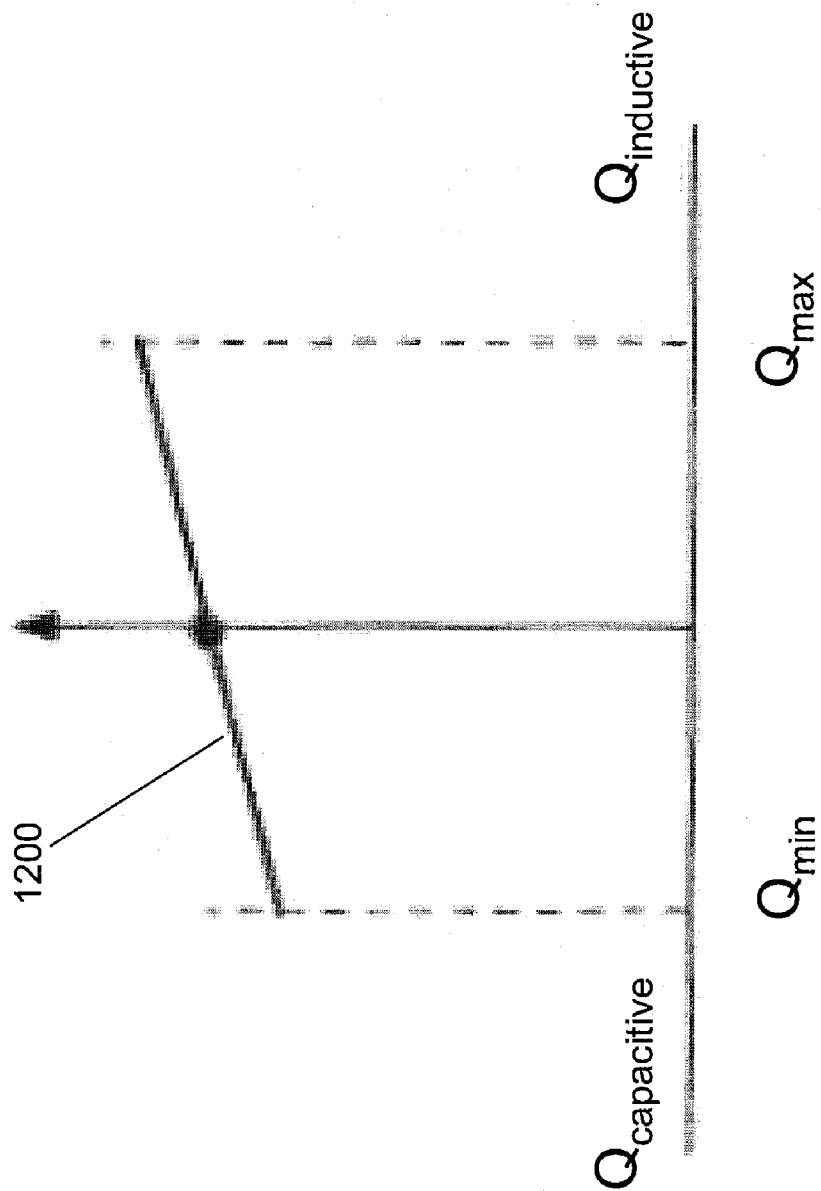


Fig. 12

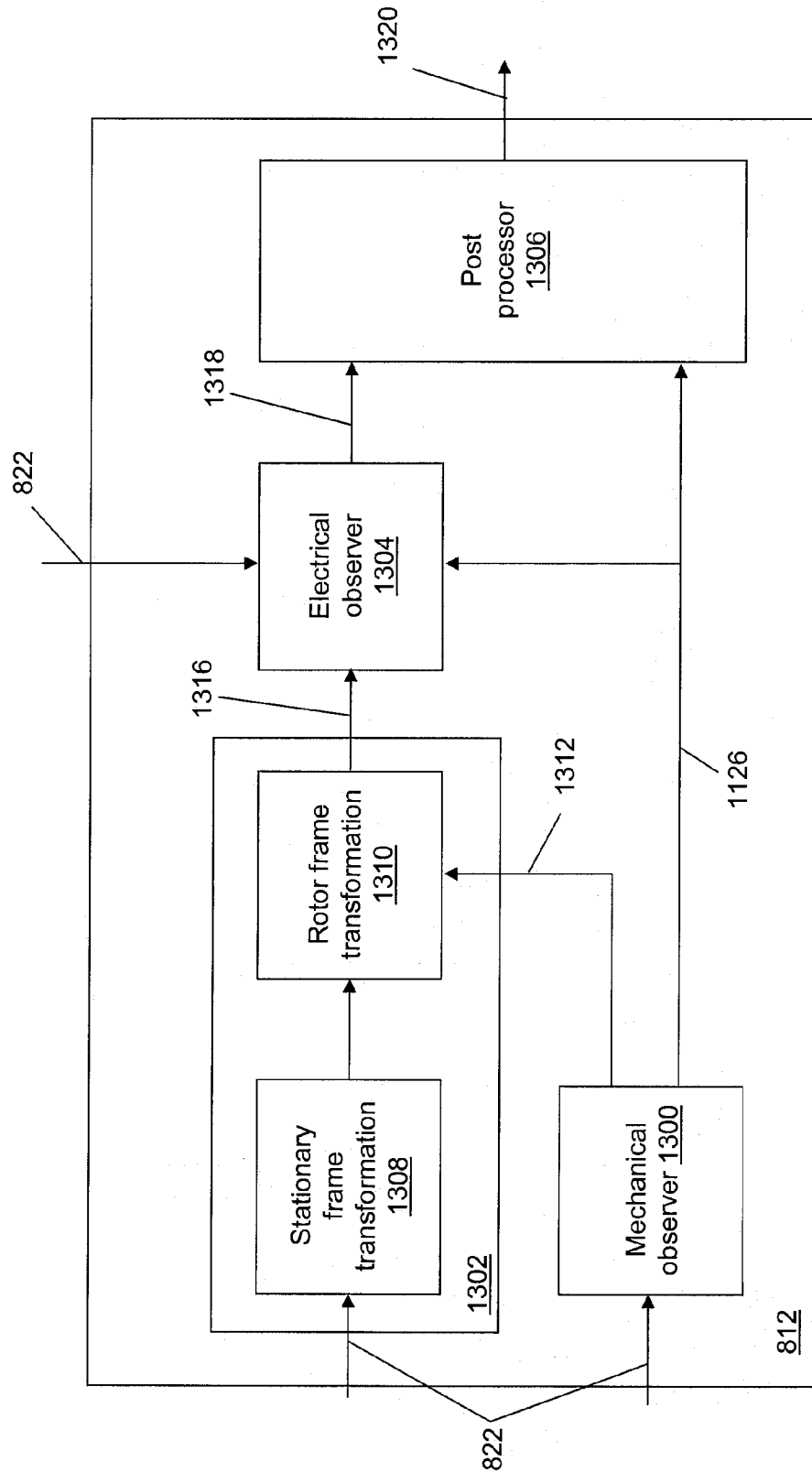


Fig. 13

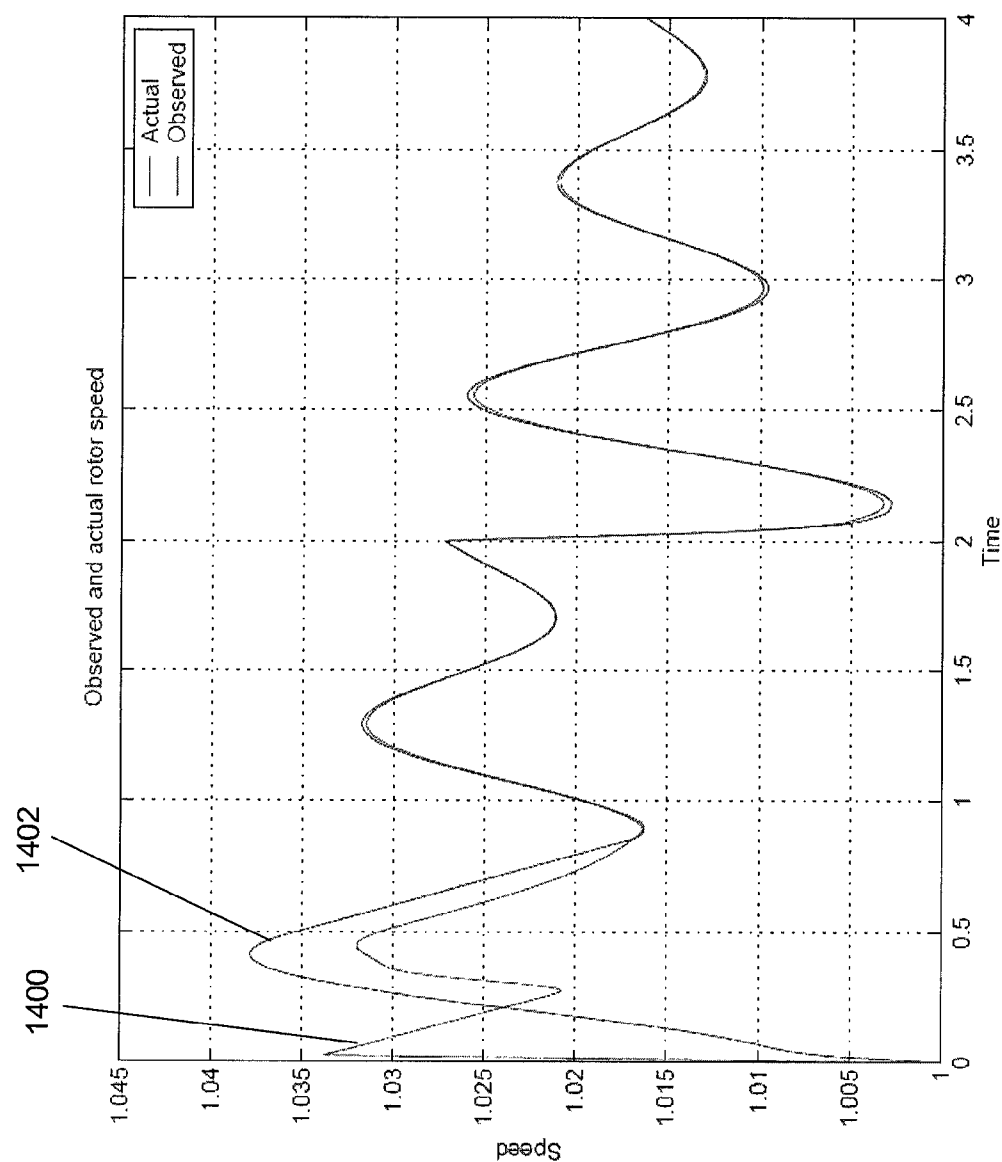


Fig. 14

1

NON-INVERTER BASED DISTRIBUTED ENERGY RESOURCE FOR USE IN A DYNAMIC DISTRIBUTION SYSTEM

REFERENCE TO GOVERNMENT RIGHTS

This invention was made with United States government support awarded by the following agencies: National Science Foundation, Electrical & Communications System Div., Award No. 0078522. The United States government has certain rights in this invention.

FIELD

The field of the disclosure relates generally to power systems. More specifically, the disclosure relates to a controller for a non-inverter based distributed energy resource used as part of a dynamic distribution system.

BACKGROUND

The demand for electrical power continues to grow worldwide. At the same time, aging transmission and distribution systems remain subject to occasional failures. Massive failures covering wide geographical areas and affecting millions of people have occurred, even in the United States, which has historically enjoyed a relatively reliable electrical power system. Problems with the capacity and reliability of the public power grid have driven the development of distributed energy resources (DER), small independent power generation systems which may be owned by, and located near, consumers of electrical power. DERs include a wide range of technologies, such as internal combustion engines, gas turbines, micro-turbines, photovoltaic cells, fuel cells, wind-power, storage systems, etc.

DERs can provide reliable power in critical applications as a backup to the primary electrical supply. For example, an interruption of power to a hospital can have life-threatening consequences. Similarly, when power to a factory is interrupted, productivity is lost, materials in process are wasted, and other costs are incurred in association with restarting the production line. Additionally, power from a DER can be provided to the main power grid to reduce energy price peaks by arbitraging energy price differentials. Geographically distributed sources of power, such as wind, solar, or hydroelectric power, may be too limited or intermittent to be used as the basis for a centralized power plant. However, these types of power sources can supplement or replace conventional power sources when the main power grid is available and can provide a backup when the main power grid is unavailable to increase energy efficiency and to reduce pollution and greenhouse gas emissions through the use of combined heat and power DER systems. DERs also can be used to meet load growth requirements and to enhance the robustness of the transmission system with a minimal addition of new lines.

DERs may be designed to operate in one of two modes: (1) "isolation" or "island" mode, wherein the DER is isolated from the main grid, and (2) normal "grid" mode, wherein the DER is connected to the main grid to either import power from or export power to the main grid. Smooth and efficient transition between the two modes is necessary to effectively integrate DERs into the distribution system without harming the integrity of the remaining system. A centralized electrical power utility is in a position to monitor and coordinate the production and distribution of power from multiple generators. In contrast, DERs may include independent producers of power who have limited awareness or communication with

2

each other. Even if the independent producers of power are able to communicate with each other, there may not be an effective way to ensure that they cooperate. As a result, to realize the potential of integrating DERs into the distribution system, the integration should not depend on complex, centralized command and control systems.

Generally speaking, DERs can include two broad categories of electrical power sources: Direct current (DC) sources, such as fuel cells, solar cells, and batteries; and high-frequency analog current (AC) sources, such as micro-turbines and wind turbines. Both types of sources are typically used to provide an intermediate DC voltage, that may be produced directly by DC sources, and produced indirectly from AC sources, for example by rectification. In both types of sources, the intermediate DC voltage is subsequently converted to AC voltage or current at the required frequency, amplitude, and phase angle for use. In most cases, the conversion from the intermediate DC voltage to the usable AC voltage is performed by a voltage inverter that can rapidly control the magnitude and phase of its output voltage.

A DER generator may be a permanent magnet or a wound field machine. The prime mover for the generator may be an engine, a turbine (gas, wind, steam, micro, etc.), a mechanical storage such as a flywheel, etc. In the case of a permanent magnet generator, the front end may consist of a rectifier feeding a DC bus which requires an inverter to interface with the AC system. The control of the inverter-based source is described, for example, in U.S. Pat. No. 7,116,010 and/or in U.S. Patent Publication No. 2006/000208574, the contents of which are incorporated by reference. Where the disclosure of the present application is limited by or in conflict with the disclosures of U.S. Pat. No. 7,116,010 and U.S. Patent Publication No. 2006/000208574, the disclosure of the present application controls. In contrast, wound field generators generally use an exciter to control the AC voltage and relative phase produced by the machine. No inverter is needed because the machine provides the AC voltage at the desired frequency as long as the speed of the shaft is kept approximately equal to a fixed value. The reduced cost of this type of system due to the absence of the power electronic front end is a significant advantage over other types of systems. However, one of the primary drawbacks of this type of system is that, without the inverter front end, the dynamics of the prime mover cannot be decoupled from the output of the generator. What is needed, therefore, is a method and a system capable of effective utilization of a non-inverter based DER system.

SUMMARY

A method and a system for effective utilization of a non-inverter based DER system are provided in an exemplary embodiment. The system responds to events using only local information available to the DER system to provide voltage regulation and power vs. frequency droop as required for use in a microgrid and as part of a public power grid. A shaft rotation speed of the prime mover is controlled using a fuel command determined based on a requested operating frequency for the system.

In an exemplary embodiment, a controller for controlling a non-inverter based distributed energy resource is provided. The controller calculates a maximum frequency change for a generator based on a comparison between a first power set point and a measured power from the generator. The controller further calculates a minimum frequency change for the generator based on a comparison between a second power set point and the measured power from the generator. The controller still further calculates an operating frequency for the

3

generator based on a comparison between a power set point and a measured power flow. A requested shaft speed for a prime mover is calculated by combining the calculated maximum frequency change, the calculated minimum frequency change, and the calculated operating frequency. A shaft speed adjustment for the prime mover is calculated based on a comparison between the calculated requested shaft speed and a measured shaft speed of the prime mover. A fuel command for the prime mover is calculated based on the calculated shaft speed adjustment to adjust a rotation rate of a shaft of the prime mover thereby controlling a frequency of an output power of the generator.

In an exemplary embodiment, a microsource is provided. The microsource includes a generator, a prime mover, and a controller. The prime mover includes a shaft connected to drive the generator to generate power at a frequency controlled by a rotation rate of the shaft. The controller calculates a maximum frequency change for the generator based on a comparison between a first power set point and a measured power from the generator. The controller further calculates a minimum frequency change for the generator based on a comparison between a second power set point and the measured power from the generator. The controller still further calculates an operating frequency for the generator based on a comparison between a power set point and a measured power flow. A requested shaft speed for the prime mover is calculated by combining the calculated maximum frequency change, the calculated minimum frequency change, and the calculated operating frequency. A shaft speed adjustment for the prime mover is calculated based on a comparison between the calculated requested shaft speed and a measured shaft speed of the prime mover. A fuel command for the prime mover is calculated based on the calculated shaft speed adjustment to adjust the rotation rate of the shaft of the prime mover thereby controlling the frequency.

In another exemplary embodiment, a method of controlling a non-inverter based distributed energy resource is provided. A maximum frequency change for a generator is calculated based on a comparison between a first power set point and a measured power from the generator. A minimum frequency change for the generator is calculated based on a comparison between a second power set point and the measured power from the generator. An operating frequency for the generator is calculated based on a comparison between a power set point and a measured power flow. A requested shaft speed for a prime mover is calculated by combining the calculated maximum frequency change, the calculated minimum frequency change, and the calculated operating frequency. A shaft speed adjustment for the prime mover is calculated based on a comparison between the calculated requested shaft speed and a measured shaft speed of the prime mover. A fuel command for the prime mover is calculated based on the calculated shaft speed adjustment. A rotation rate of a shaft of the prime mover is adjusted based on the calculated fuel command to control a frequency of an output power of the generator.

Other principal features and advantages of the invention will become apparent to those skilled in the art upon review of the following drawings, the detailed description, and the appended claims.

BRIEF DESCRIPTION OF THE DRAWINGS

Exemplary embodiments of the invention will hereafter be described with reference to the accompanying drawings, wherein like numerals denote like elements.

4

FIG. 1 depicts a block diagram of a distributed energy resource system in accordance with an exemplary embodiment.

FIG. 2 is a diagram of a microgrid that includes a microsource implementing a unit power control scheme in accordance with an exemplary embodiment.

FIG. 3 is a diagram of a microgrid that includes a microsource implementing a zone power control scheme in accordance with an exemplary embodiment.

FIG. 4 is a graph depicting the relationship between steady state unit power vs. frequency ($P-\omega$) for two exemplary microsources having different loads for use in a unit power control scheme in accordance with an exemplary embodiment.

FIG. 5 is a graph depicting the relationship between steady state zone power vs. frequency ($F-\omega$) for two exemplary microsources having different loads for use in a zone power control scheme in accordance with an exemplary embodiment.

FIG. 6 is a diagram of two microsources used in a single zone in accordance with an exemplary embodiment.

FIG. 7 is a diagram of two microsources used in multiple zones in accordance with an exemplary embodiment.

FIG. 8 is a block diagram of a controller for a non-inverter based distributed energy resource in accordance with an exemplary embodiment.

FIG. 9 is a block diagram of a voltage regulator of the controller of FIG. 8 in accordance with an exemplary embodiment.

FIG. 10 is a graph depicting a sliding window for applying generating power limits in accordance with an exemplary embodiment.

FIG. 11 is a block diagram of a $P-\omega$ droop governor of the controller of FIG. 8 in accordance with an exemplary embodiment.

FIG. 12 is a graph of an voltage droop regulation characteristic for a voltage regulator in accordance with an exemplary embodiment.

FIG. 13 is a block diagram of an observer used with the controller of FIG. 8 in accordance with an exemplary embodiment.

FIG. 14 is a graph comparing an actual rotor speed with an observed rotor speed determined using the observer of FIG. 13 in accordance with an exemplary embodiment.

DETAILED DESCRIPTION

With reference to FIG. 1, a distributed energy resource (DER) system 100 is shown in accordance with an exemplary embodiment. Such an exemplary system is described, for example, in U.S. Pat. No. 7,116,010 and/or in U.S. Patent Publication No. 2006/000208574. DER system 100 may include a utility supply 102 connected to a feeder line 104 that interconnects one or more microsource systems 106a, 106b, 106c, and 106d and one or more loads 108a, 108b, and 108c. DER system 100 may include a plurality of feeder lines. Feeder line 104, the one or more microsource systems 106a, 106b, 106c, and 106d, and the one or more loads 108a, 108b, and 108c can form a microgrid 110. Utility supply 102 can connect microgrid 110 to other similar microgrids distributed throughout DER system 100. A microsource system can include exemplary microsource power sources, power storage, and power controllers. The power source can be, for example, a fuel cell, hydroelectric generator, photovoltaic array, windmill, microturbine, etc. The power storage, if present, can be, for example, a battery or flywheel.

5

Feeder line **104** may include one or more interface switches. An exemplary interface switch is described, for example, in U.S. patent application Ser. No. 11/266,976, filed Nov. 4, 2005 and entitled INTERFACE SWITCH FOR DISTRIBUTED ENERGY RESOURCES, the contents of which are incorporated by reference. Where the disclosure of the present application is limited by or in conflict with the disclosure of U.S. patent application Ser. No. 11/266,976, the disclosure of the present application controls. The interface switch, if used, can be positioned between feeder line **104** and utility supply **102** so that microgrid **110** can be isolated from utility supply **102**. When microgrid **110** is isolated from utility supply **102**, the microgrid **110** is said to be operating in “island mode”. When microgrid **110** is connected to the utility supply **110**, the microgrid **110** is said to be operating in “grid mode”. When DER system **100** is connected to the grid, the one or more loads **108a**, **108b**, and **108c** may receive power from both the grid and local sources, depending on the current situational demands.

When a microsource or microgrid operates in island mode, load tracking problems can arise because typical power sources used in microsources, such as microturbines or fuel cells, tend to respond slowly, with time constants ranging from 10 to 200 seconds. Additionally, these types of power sources may be inertialess. Conventional utility power systems store energy in the inertia of the spinning mass of a generator. When a new load comes online, the initial energy balance can be met by the system’s inertia, which results in a slight reduction in system frequency. Because power sources in microsources may be inertialess, a microsource may include power storage to ensure initial energy balance when loads are added during island mode.

Each microsource system **106a**, **106b**, **106c**, and **106d** preferably includes a microsource controller. The microsource controller responds to events using local information to respond to voltage drops, faults, blackouts, etc. and to switch to island operation mode as needed. The microsource controller controls the change in the output power of the system components as they change from a dispatched power mode to one in which frequency is controlled and load following is provided. Control schemes for a power controller in DER system **100** can be classified into one of three broad classes: unit power control, zone power control, and a mixed system using both unit power control and zone power control. Using a unit power controller, load changes are matched by a corresponding power injection from the utility because a microsource holds its injection to a set point P_o . During island mode, the microsource matches the power demand as loads change. Each microsource system **106a**, **106b**, **106c**, and **106d** regulates the voltage magnitude at its connection point and the injected power using either a variable slope method or a fixed slope method.

Using a zone power controller, power flow in zones is controlled instead of controlling the power flow from each microsource. Each microsource system **106a**, **106b**, **106c**, and **106d** regulates the voltage magnitude at its connection point and the power that is flowing in the feeder. Using a zone power controller, the microsource systems **106a**, **106b**, **106c**, and **106d** pick-up extra load demands, and as a result, show a constant load to the utility grid. In this case, DER system **100** becomes a true dispatchable load as seen from the utility side supporting demand-side management arrangements. To reduce confusion, the symbol, F , is used for power flow in a zone and the symbol, P , is used for the power output from a microsource. When connected to the grid, load changes are matched by a different power injection from the microsource because the controller holds the flow of power coming from

6

the grid, F_{line} , to a constant value. During island mode, all of the microsources participate in matching the power demand as loads change.

With reference to FIG. 2, a diagram of a microgrid **200** is shown in accordance with an exemplary embodiment using a unit power controller. Microgrid **200** may include a microsource **202** and a load **108**. Microsource **202** may be connected to feeder line **104** by an inductor **204**. An interface switch may be provided, for example, in feeder line **104**. The interface switch can be opened to isolate microgrid **200** from the rest of DER system **100** and can be closed to connect microgrid **200** to the rest of DER system **100**. Microsource **202** may include a controller capable of measuring a current through inductor **204** and of measuring a system voltage at a point **206** in feeder line **104** where inductor **204** joins feeder line **104**.

With reference to FIG. 3, a diagram of a microgrid **300** is shown in accordance with an exemplary embodiment using a zone power controller. Microgrid **300** may include a microsource **302** and load **108**. Microsource **302** may be connected to feeder line **104** by inductor **204**. An interface switch may be provided, for example, in feeder line **104**. The interface switch can be opened to isolate microgrid **300** from the rest of DER system **100** and can be closed to connect microgrid **300** to the rest of DER system **100**. Microsource **302** may include a controller capable of measuring a current at a point **304** in feeder line **104** between utility supply **102** and inductor **204** and of measuring a system voltage at a point **206** in feeder line **104** where inductor **204** joins feeder line **104**.

With reference to FIG. 4, a graph depicting the relationship between steady state unit power and frequency ($P-\omega$) using a fixed minimum slope method and unit power control is shown in accordance with an exemplary embodiment. FIG. 4 shows steady state characteristics. The response may deviate from the characteristic during a transition period. Two exemplary microsources included in the microgrid are shown. The microsources have different power set points though this is not required. A first microsource has a first power set point **402**. A second microsource has a second power set point **404**. First power set point **402** and second power set point **404** are the amount of power injected by each source when connected to the grid at a system frequency ω_o . A constant slope

$$m = -\frac{\Delta\omega}{P_{max}}$$

allows power to change between $P=0$ and $P=P_{max}$ as frequency changes over $\Delta\omega$. A lower bounding line **400** extends from $P=0$ to $P=P_{max}$ with a starting frequency of ω_o . An upper bounding line **401** extends from $P=0$ to $P=P_{max}$ with a starting frequency of $\omega_o + \Delta\omega$. Because a constant slope is used by the controller, the response lines are all parallel to and extend between lower bounding line **400** and upper bounding line **401**.

Movement along the lines of constant slope m in response to a transition to island mode depends on whether or not the microgrid is importing power from or exporting power to the grid. If the system was exporting to the grid before islanding, the resulting frequency of ω_{exp} **412** is greater than the system frequency ω_o . For example, if the system was exporting to the grid before islanding, the second microsource may move from the system frequency ω_o at second power set point **404** to a third power set point **410** operating at ω_{exp} **412**. The first microsource may shift from the system frequency ω_o at first

7

power set point **402** to a fourth power set point **406** at $P=0$. When the $P=0$ limit is reached, the slope of the characteristic is switched to vertical, as shown by the arrows, to move the first microsource frequency upwards to a fifth power set point **408** operating at ω_{exp} **412**. The specific set points, of course, depend on the local demands and operating points of the microsources. A $P=0$ limit may not be reached by either microsource.

If the system was importing from the grid before islanding, the resulting frequency of ω_{imp} **420** will be smaller than the system frequency ω_o . For example, if the system was importing to the grid before islanding, the first microsource may move from the system frequency ω_o at first power set point **402** to a sixth power set point **414** operating at ω_{imp} **420**. The second microsource may move from the system frequency ω_o at second power set point **404** to a seventh power set point **416** at $P=P_{max}$. When the $P=P_{max}$ limit is reached, the slope of the characteristic is switched to vertical, as shown by the arrows, to move the second microsource frequency downwards to an eighth power set point **418** operating at ω_{imp} **420**. The minimum and maximum power limits are enforced by switching the characteristic with constant slope to a vertical steady state characteristic when the minimum or maximum power limit is reached. The specific set points, of course, depend on the local demands and operating points of the microsources. A $P=P_{max}$ limit may not be reached by either microsource.

With reference to FIG. 5, a graph depicting the relationship between steady state zone power and frequency ($F-\omega$) using a fixed minimum slope method and zone power control is shown in accordance with an exemplary embodiment. Two exemplary microsources are included in the microgrid. The microsources have different power set points. A first microsource has a first flow set point **500**. A second microsource has a second flow set point **502**. The slope is fixed at the minimum slope m , but has a reversed sign because of the relation between the microsource output power, P , and the zone power flow, F , which can be derived by inspection of FIG. 3 as $F_{line} + P_{source} = \text{Load}$. F_{line} is the power (imported means positive) from the rest of DER system **100**, and P_{source} is the power injected or absorbed by microsource **302**. The power injected or absorbed by microsource **302** is assumed to be greater than the minimum power output, P_{min} , of microsource **302** and less than the maximum power output, P_{max} , of microsource **302**. For a microsource capable of power injection only, P_{min} is positive or zero, while a bidirectional device capable of both power injection or power storage may have $P_{min} < 0$. Load is the overall loading level seen by microsource **302**.

During connection with the grid, the flow in the zones tracks the requested values at the system frequency ω_o . When the microgrid transfers to island mode, the two microsources readjust the flow depending on the arrangement of the microsources with respect to each other and utility supply **102**. When regulating unit power, the relative location of loads and microsources is irrelevant, but when regulating zone power flow, the relative location of loads and microsources is important. For example, with reference to FIG. 6, a first microsource **604** and a second microsource **610** are arranged in series in a single zone. The use of a single zone is for illustrative purposes only. There can be a greater or a lesser number of microsources in a single zone.

The zone includes a first load **606** and a second load **612** on a local power bus **614** connected by an interface switch **600** to utility supply **102**. During a transition to island mode, interface switch **600** opens. As a result, in a zone power control method for the circuit of FIG. 6, a first flow **602** nearest to the utility system is zero in island mode. A second flow **608** may

8

increase to compensate for the first flow **602** transition to zero. Thus, with reference to FIG. 5, first flow **602** moves from the system frequency ω_o at first flow set point **500** to a third flow set point **510** operating at the frequency ω_{exp} **514**. Second flow **608** moves from the system frequency ω_o at second flow set point **502** to a fourth power set point **512**. As a result, in island mode, the system operates at frequency ω_{exp} **514** where first flow **602** is zero. Frequency ω_{exp} **514** is larger than the nominal system frequency ω_o because the system was exporting to the grid ($|\text{first flow } 602| < |\text{second flow } 608|$), which is the same behavior seen using unit power control.

With reference to FIG. 7, a first microsource **706** and a second microsource **710** are arranged in parallel in two zones. The use of two zones each with a single microsource is for illustrative purposes only. There can be a greater or a lesser number of microsources in a greater or a lesser number of zones. A first load **708** is located on a first local power bus **714** connected by an interface switch **700** to utility supply **102**. A second load **712** is located on a second local power bus **716** connected by interface switch **700** to utility supply **102**. A first flow **702** flows through first local power bus **714**, and a second flow **704** flows through second local power bus **716**. The grid flow is the algebraic sum of first flow **702** and second flow **704**. During a transition to island mode, interface switch **700** opens.

In a zone power control method for the arrangement of FIG. 7, during island mode, the frequency takes the value where the sum of the flows is zero. As a result as shown on FIG. 5, the frequency in island mode is frequency ω_{par} **508** where $F1 = -F2$. With reference to FIG. 5, first flow **702** moves from the system frequency ω_o at first flow set point **500** to a fifth flow set point **504** operating at the frequency ω_{par} **508**. Second flow **704** moves from the system frequency ω_o at second flow set point **502** to a sixth power set point **506** at the frequency ω_{par} **508**.

With reference to FIG. 8, a non-inverter based microsource system **800** is shown in accordance with an exemplary embodiment. Microsource system **800** and its various components may be implemented in or include hardware, firmware, software, or any combination of these methods. Thus, microsource system **800** may include circuitry that can implement the processes indicated in the form of hardware, firmware, and/or a processor executing instructions embodied in software. Microsource system **800** connects to a grid through feeder lines **802**. Feeder lines **802** extend toward utility supply **102** in a first direction **804** and away from utility supply **102** in a second direction **806**. Microsource system **800** connects to feeder lines **802** through bus lines **803**. Microsource system **800** may include an observer **812**, a voltage regulator **814**, a $P-\omega$ droop governor **816**, a prime mover **818**, a field controlled generator **820**, and a transformer **840**. A first sensor may measure a three phase feeder current **808** through feeder lines **802**. A second sensor may measure a three phase feeder bus voltage **810** at the connection point of bus lines **803** with feeder lines **802**. A third sensor may measure a three phase bus current **809** through bus lines **803** between transformer **840** and feeder lines **802**.

Field controlled generator **820** connects to feeder lines **802** through transformer **840**. Field controlled generator **820** may be directly connected to the grid. As a result, transformer **840** need not be included in microsource system **800**. For example, if the internal reactance is large enough to achieve the necessary isolation, transformer **840** is not needed. It is well known to drive a generator with a prime mover attached to the rotor shaft of the generator. Typically, the electrical output provided by the generator is responsive to the excitation of a field coil in the generator. Fuel is combusted in prime

mover **818** to cause an output shaft to turn at a rotational speed or frequency ω_{shaft} which in turn drives the frequency of the generator output.

Observer **812** captures local measurements **822** for input to voltage regulator **814** and P- ω droop governor **816**. Local measurements **822** may include feeder current **808**, feeder bus voltage **810**, bus current **809**, the angular velocity or frequency of the shaft ω_{shaft} of field controlled generator **820**, a rotor position, etc. Observer **812** uses electrical measurements of current and voltage and measurements of ω_{shaft} to calculate data needed by voltage regulator **814** and a P- ω droop governor **816**. Voltage regulator **814** may utilize a plurality of inputs **826**. P- ω droop governor **816** may utilize a plurality of inputs **830**. An exemplary observer is discussed further with reference to FIG. 13.

Voltage regulator **814** assists in decoupling interactions between DER microsources and includes a voltage vs. reactive power droop controller so that, as the reactive power Q generated by field controlled generator **820** becomes more capacitive, a local voltage set point **824** is reduced. Conversely, as Q becomes more inductive, the local voltage set point **824** is increased. P- ω droop governor **816** provides the P- ω and/or F- ω functions described with reference to FIGS. 4 and 5. P- ω droop governor **816** additionally provides control over prime mover **818**. Prime mover **818** can be, for example, an engine, micro turbine, wind turbine, mechanical storage, etc.

With reference to FIG. 9, a block diagram of voltage regulator **814** is shown in accordance with an exemplary embodiment. Voltage regulator **814** may include a β block **900**, a first summer **902**, a second summer **904**, and a controller **906**. The local voltage set point **824** is input to voltage regulator **814**. A regulated output voltage **828** is output from voltage regulator **814** and input to field controlled generator **820**. Creating an appropriate regulated output voltage at the terminals of field controlled generator **820** regulates feeder bus voltage **810**. A reactive power Q **908** may be calculated by observer **812**, for example, using the measured feeder bus voltage **810** and the measured bus current **809** as inputs. Reactive power Q **908** is input to β block **900**, which calculates a modified reactive power **912**. A terminal voltage **910** may be calculated by observer **812** and input to voltage regulator **814**.

The modified reactive power **912** is subtracted from local voltage set point **824** in first summer **902** to define a desired local voltage set point **914** based on a droop constant β defined in β block **900**. In an exemplary embodiment, β block **900** is implemented to exhibit a voltage vs. reactive current droop as shown with reference to FIG. 12. Droop constant β is the slope of the droop characteristic line **1200**. As reactive power Q becomes more inductive, the desired local voltage set point **914** becomes larger than the local voltage set point **824**. As reactive power Q becomes more capacitive, the desired local voltage set point **914** becomes smaller than the local voltage set point **824**. Terminal voltage **910** is compared to the desired local voltage set point **914** in second summer **904**. For example, terminal voltage **910** is subtracted from the desired local voltage set point **914**. The resulting voltage error **916** is input to controller **906** to generate the regulated output voltage **828**. In an exemplary embodiment, controller **906** is a proportional-integral controller.

Field controlled generator **820** can operate in flow control mode with an F- ω characteristic as shown in FIG. 5 or in unit power control mode with a P- ω characteristic as shown in FIG. 4. In either case, the limits of power from field controlled generator **820** are used. With reference to FIG. 10, the range of output power, P, available from field controlled generator **820** imposes a window **1007** on feeder flow, F, such that

$P_{load} - P_{max} < F < P_{load} - P_{min}$, where P_{load} is the load on the system, and P_{max} and P_{min} are the power limits of field controlled generator **820**. A system F- ω_o operating point **1000** is defined for the system frequency ω_o . The limits for the feeder flow, F, can be visualized on the F- ω plane as a window whose width **1006** is the difference between F_{min} **1002** and F_{max} **1004** which equals the difference between P_{max} and P_{min} . The location of the window on the F-axis depends on the value of P_{load} . As P_{load} increases, window **1007** slides to the right on the F- ω plane. Conversely, if the load is reduced, window **1007** slides to the left on the F- ω plane.

An example flow set point **1008** falls within window **1007**. Situations are possible that can result in the flow set point falling outside window **1007**. For example, load levels while connected to the grid, an incorrect choice for the flow set point, a change in output power of other microsources, and a transfer to island mode all can cause the flow set point to fall outside window **1007**. For example, a first flow set point **1010** falls to the left of window **1007**. In this situation, P_{max} is exceeded. As another example, a second flow set point **1012** falls to the right of window **1007**. In this situation, P_{min} is exceeded. To avoid a flow set point falling outside window **1007**, when the flow set point is outside window **1007**, the controls reset the flow set point to the closest edge of window **1007**.

With reference to FIG. 11, P- ω droop governor **816** is shown in accordance with an exemplary embodiment. P- ω droop governor **816** may include a mode switch block **1100**, a first summer **1102**, a first proportional-integral (PI) controller **1104**, a second summer **1106**, a second PI controller **1108**, a fuel controller block **1110**, a third summer **1112**, a multiplier **1114**, a fourth summer **1116**, a fifth summer **1118**, and a sixth summer **1120**. The plurality of inputs **830** from observer **812** to P- ω droop governor **816** may include a three phase power P **1122**, a three phase grid power flow F **1124**, and an angular velocity or revolutions per minute of the shaft, ω_{shaft} **1126** of field controlled generator **820**. With reference to FIG. 8, inputs of P- ω droop governor **816** also include power limits **834**, a power set point **832**, and a frequency set point **833**. Outputs of P- ω droop governor **816** include a fuel command **836** input to prime mover **818**.

With reference to FIG. 11, P- ω droop governor **816** may be used to provide zone power control or unit power control. As a result, power set point **832** may be P_o or F_o . If unit power control is used, power flow **1142** is three phase power P **1122**. If zone power control is used, power flow **1142** is three phase grid power flow F **1124**. Mode switch **1100** determines which power parameter, three phase power P **1122** or three phase grid power flow F **1124**, is input to third summer **1112**. If unit power control is used, the sign of slope m in multiplier block **1114** is reversed.

Three phase power P **1122** is input to first summer **1102** and second summer **1106**. Power limits **834** include a P_{max} set point **1130** of field controlled generator **820** and a P_{min} set point **1136** of field controlled generator **820**. Changing the limits P_{max} and P_{min} controls the width of window **1007** shown with reference to FIG. 10. First summer **1102** compares P_{max} set point **1130** with three phase power P **1122** to calculate a first power difference **1132** input to first PI controller **1104**. For example, first summer **1102** subtracts three phase power P **1122** from P_{max} set point **1130** so that first power difference **1132** is negative if the P_{max} set point **1130** is exceeded. First PI controller **1104** controls the maximum power through a maximum frequency change **1134**, $\Delta\omega_{max}$, that is limited between a minimum frequency and 0 Hz. In an exemplary embodiment, the minimum frequency is -1 Hz. Second summer **1106** compares P_{min} set point **1136** with three

11

phase power **P 1122** to calculate a second power difference **1138** input to second PI controller **1108**. For example, second summer **1106** subtracts three phase power **P 1122** from P_{min} set point **1136** so that second power difference **1138** is positive if the P_{min} set point **1136** is exceeded. Second PI controller **1108** controls the minimum power through a minimum frequency change **1140**, $\Delta\omega_{min}$, that is limited between 0 Hz and a maximum frequency. In an exemplary embodiment, the maximum frequency is 1 Hz. $\Delta\omega_{max}$ and $\Delta\omega_{min}$ are scaled as radians for input to fifth summer **1118**. In general, control parameters of the first and second PI controllers **1104**, **1108** are set such that a steady state at a limit is reached in 10-20 cycles. Maximum frequency change **1134** and minimum frequency change **1140** maintain the flow set point within window **1007**.

Third summer **1112** compares power set point **832** with power flow **1142** (three phase grid power flow **F 1124** or three phase power **P 1122** depending on the type of power control used as determined by mode switch **1100**) to calculate a third power difference **1144** input to multiplier **1114**. For example, third summer **1112** subtracts power flow **1142** from power set point **832**. Multiplier **1114** multiplies third power difference **1144** by the slope m to determine a frequency change **1146**. Depending on the type of power control, frequency change **1152** may be defined as $m(F_o - F)$ or $-m(P_o - P)$.

Fourth summer **1116** adds frequency set point **833** to frequency change **1146** to calculate an operating frequency **1148** input to fifth summer **1118**. Fifth summer **1118** adds operating frequency **1148** with maximum frequency change **1134** and minimum frequency change **1140** to calculate a requested shaft speed **1150** input to sixth summer **1120**. Sixth summer **1120** compares ω_{shaft} **1126** with requested shaft speed **1150** to calculate a shaft rotation error **1152** input to fuel controller **1110**. For example, sixth summer **1120** subtracts ω_{shaft} **1126** from requested shaft speed **1150** to determine shaft rotation error **1152**. The output of fuel controller **1110** is fuel command **836** for prime mover **818**, which is calculated based on shaft rotation error **1152**. In an exemplary embodiment, fuel controller **1110** is a proportional-integral controller. As known to those skilled in the art, can be implemented using a fewer or a greater number of elements than those depicted in FIGS. 8, 9, and 11. The elements shown are merely exemplary.

Through the operations of voltage regulator **814** and P- ω droop governor **816** effective utilization of a non-inverter based DER system is provided. A fuel command **836** is determined which controls prime mover **818** of field controlled generator **820** to provide voltage regulation and power vs frequency droop as necessary to effectively utilize a non-inverter based DER system in the microgrid.

With reference to FIG. 13, a block diagram of observer **812** is shown in accordance with an exemplary embodiment. Observer **812** may include a mechanical observer **1300**, a Blondel-Park transformation block **1302**, an electrical observer **1304**, and a post processor block **1306** to estimate the state of microsource system **800**. Blondel-Park transformation block **1302** may include stationary frame transformation block **1308** and a rotor frame transformation block **1310**. Inputs **822** include feeder current **808**, bus current **809**, and feeder bus voltage **810** to Blondel-Park transformation block **1302**; a sampled ω_{shaft} , a sampled rotor position, and fuel command **836** to mechanical observer **1300**; and regulated output voltage **828** to electrical observer **1304**. Mechanical observer **1300** implements a closed loop observer to calculate a rotor angle **1312** input to rotor frame transformation block **1310** and to calculate ω_{shaft} **1126** input to electrical observer **1304** and post processor block **1306** using the sampled ω_{shaft} .

12

the sampled rotor position, and fuel command **836**. Using Blondel-Park transformation block **1302** and rotor angle **1312**, the voltages and currents are transformed to a reference frame situated on the rotor of generator **820**. The transformed quantities **1316** are input to electrical observer **1304** to generate electrical states **1318** of microsource system **800**. Post processor **1306** generates output quantities **1320** needed by voltage regulator **814** and P- ω droop governor **816**. The output quantities **1320** may include reactive power **Q 908**, terminal voltage **910**, three phase power **P 1122**, three phase grid power flow **F 1124**, and ω_{shaft} **1126**.

An initial rotor angle may be obtained utilizing the fact that, during no load, the terminal voltage is equal to the back electromotive force of generator **820**. Thus, at no load, the rotor angle is the arc tangent of

$$\frac{V_{ds}}{V_{qs}}$$

To initialize the rotor angle, generator **820** is started with no load. A terminal voltage is measured and a rotor angle calculated. An input electrical power is calculated using the measured terminal voltages and currents. Mechanical observer **1300** is executed closed loop using a sampled ω_{shaft} , the calculated rotor angle, and an input fuel command **836** to estimate ω_{shaft} **1126**. ω_{shaft} **1126** is compared with the sampled ω_{shaft} to calculate a speed error. When the speed error falls below a tolerance value, observer **812** has locked on to the correct rotor speed and rotor angle. After locking on to the correct rotor speed and rotor angle, an integral of ω_{shaft} **1126** input to observer **812** provides rotor angle **1312** output from mechanical observer **1300**, and the load can be applied to generator **820**.

An additional loop to provide a zero steady state rotor angle estimation error can be included which uses a resolver on the shaft of generator **820**. The output of the resolver is processed to obtain the rotor position. The initial rotor angle again is the arc tangent of

$$\frac{V_{ds}}{V_{qs}}$$

The resolver output is correlated with the rotor angle to calculate an angle offset. The resolver output can be used to determine rotor angle **1312** based on the angle offset calculated.

Blondel-Park transformation block **1302** employs a dq-transformation as known to those skilled in the art. The dq-transformation is used to reference the current and voltages to a common reference frame. The dq-transformation can be split in two steps. First, the original three-phase variables (currents, voltages, and/or magnetic fluxes) are transformed to a stationary reference frame in stationary frame transformation block **1308**. For three-phase systems in equilibrium, this transformation results in two transformed components because the third component (the homopolar) is zero for any balanced set and is decoupled from the remaining dynamic equations. Second, the transformed variables from stationary frame transformation block **1308** are transformed to the rotating rotor reference frame in rotor frame transformation block **1310** to determine the transformed quantities **1316**.

13

Electrical observer **1304** receives rotor speed **1314** and the transformed quantities **1316** and executes the following equations, which describe the electrical system:

$$\psi_{md}^r = \frac{\frac{\psi_{kb}^r}{x_{lkd}} + \frac{\psi_{fd}^r}{x_{lfd}} + i_{ds}}{\frac{1}{x_{md}} + \frac{1}{x_{lkd}} + \frac{1}{x_{lfd}}}$$

$$p\psi_{kd}^r = \omega_b r_{kd} \left(\frac{\psi_{md}^r - \psi_{kd}^r}{x_{lkd}} \right)$$

$$pE_f = \frac{-E_f + V_V}{T_e}$$

$$p\psi_{fd}^r = \omega_b \left[E_f \frac{r_{fd}}{x_{mfd}} + r_{fd} \left(\frac{\psi_{md}^r - \psi_{fd}^r}{x_{lfd}} \right) \right]$$

$$\psi_{mq}^r = \frac{\frac{\psi_{kq}^r}{x_{lkq}} + i_{qs}}{\frac{1}{x_{mq}} + \frac{1}{x_{lkq}}}$$

$$p\psi_{kq}^r = \omega_b r_{kq} \left(\frac{\psi_{mq}^r - \psi_{kq}^r}{x_{lkq}} \right)$$

$$T_{mech} = 1.6m_f(t - T_d) - \frac{0.36}{\omega_r(t)}$$

$$p\omega_t = \frac{T_e + T_{mech}}{2H}$$

$$p\delta = \omega_b \omega_t$$

$$\psi_{qs}^r = \frac{\frac{x_{MQ}}{x_{lkq}} \psi_{kq}^r + x_{ls} i_{qs}}{1 - \frac{x_{MQ}}{x_{ls}}}$$

$$\psi_{ds}^r = \frac{\frac{x_{MD}}{x_{lkd}} \psi_{kd}^r + \frac{x_{MD}}{x_{lfd}} \psi_{fd}^r + x_{ls} i_{ds}}{1 - \frac{x_{MD}}{x_{ls}}}$$

where x_{ls} is the armature leakage reactance, x_{lkd} is the D-axis damper leakage reactance, x_{lkq} is the Q-axis damper leakage reactance, x_{lfd} is the field leakage reactance, x_{md} is the D-axis mutual reactance, x_{mq} is the Q-axis mutual reactance, ψ_{kd}^r is the D-axis damper flux voltage, ψ_{kq}^r is the Q-axis damper flux voltage, ψ_{fd}^r is the D-axis field flux voltage, T_e is the brushless exciter time constant, H is the inertia of generator **820**, and ω_b is the base frequency in radians per second.

Equations [1]-[11] provide an estimation of the states of generator **820** in real-time. Postprocessor **1306** receives electrical states **1318** and rotor speed **1314** and calculates terminal voltage V_t **910** (equation [14]), three phase power P **1122** (equation [15]), reactive power Q **908** (equation [16]), and three phase grid power flow F **1124** (equation [17]) as shown below.

$$V_{qs}^r = r_s i_{qs}^r + \omega_b \psi_{ds}^r$$

$$V_{ds}^r = r_s i_{ds}^r - \omega_b \psi_{qs}^r$$

$$V_t = \sqrt{V_{ds}^2 + V_{qs}^2}$$

$$P = V_{qs}^r i_{qs}^r + V_{ds}^r i_{ds}^r$$

$$Q = V_{ds}^r i_{qs}^r - V_{qs}^r i_{ds}^r$$

$$F = V_{qs}^r i_{qf}^r + V_{ds}^r i_{df}^r$$

14

A simulation was developed to verify observer **812**. Simulation results for the actual and observed rotor speed are shown with reference to FIG. **14** for a step change in load from no load to a load of 4 kilowatts. An observed rotor speed curve **1400** tracks an actual rotor speed curve **1402**.

The foregoing description of exemplary embodiments of the invention have been presented for purposes of illustration and of description. It is not intended to be exhaustive or to limit the invention to the precise form disclosed, and modifications and variations are possible in light of the above teachings or may be acquired from practice of the invention. The embodiments were chosen and described in order to explain the principles of the invention and as practical applications of the invention to enable one skilled in the art to utilize the invention in various embodiments and with various modifications as suited to the particular use contemplated. It is intended that the scope of the invention be defined by the claims appended hereto and their equivalents.

What is claimed is:

1. A controller for controlling a non-inverter based distributed energy resource, the controller comprising circuitry to:
 - calculate a maximum frequency change for a generator based on a first comparison between a first power set point and a measured power from the generator;
 - calculate a minimum frequency change for the generator based on a second comparison between a second power set point and the measured power from the generator;
 - calculate an operating frequency for the generator based on a third comparison between a power set point and a measured power flow;
 - calculate a requested shaft speed for a prime mover by combining the calculated maximum frequency change, the calculated minimum frequency change, and the calculated operating frequency;
 - calculate a shaft speed adjustment for the prime mover based on a fourth comparison between the calculated requested shaft speed and a measured shaft speed of the prime mover; and
 - calculate a fuel command for the prime mover based on the calculated shaft speed adjustment to adjust a rotation rate of a shaft of the prime mover thereby controlling a frequency of an output power of the generator.

2. The controller of claim 1, wherein calculation of the operating frequency comprises use of $m(F_o - F)$, where m is a slope of an F - ω characteristic, F_o is the power set point, and F is the measured power flow.

3. The controller of claim 1, wherein calculation of the operating frequency comprises use of $m(P_o - P)$, where m is a slope of a P - ω characteristic, P_o is the power set point, and P is the measured power flow.

4. The controller of claim 3, wherein the measured power is the measured power flow.

5. The controller of claim 1, wherein calculation of the maximum frequency change comprises subtracting the measured power from the first power set point to determine a power differential.

6. The controller of claim 5, wherein calculation of the maximum frequency change further comprises applying the determined power differential to a proportional-integral controller.

7. The controller of claim 1, wherein calculation of the minimum frequency change comprises subtracting the measured power from the second power set point to determine a power differential.

15

8. The controller of claim 7, wherein calculation of the minimum frequency change further comprises applying the determined power differential to a proportional-integral controller.

9. The controller of claim 1, further comprising circuitry to regulate an output voltage of the generator using a voltage versus reactive power droop controller.

10. The controller of claim 1, wherein the first power set point is a maximum and further wherein the second power set point is a minimum.

11. A method of controlling a non-inverter based distributed energy resource, the method comprising:

calculating a maximum frequency change for a generator based on a first comparison between a first power set point and a measured power from the generator;

calculating a minimum frequency change for the generator based on a second comparison between a second power set point and the measured power from the generator;

calculating an operating frequency for the generator based on a third comparison between a power set point and a measured power flow;

calculating a requested shaft speed for a prime mover by combining the calculated maximum frequency change, the calculated minimum frequency change, and the calculated operating frequency;

calculating a shaft speed adjustment for the prime mover based on a fourth comparison between the calculated requested shaft speed and a measured shaft speed of the prime mover;

calculating a fuel command for the prime mover based on the calculated shaft speed adjustment; and

adjusting a rotation rate of a shaft of the prime mover based on the calculated fuel command to control a frequency of an output power of the generator.

12. The method of claim 11, wherein calculating the operating frequency comprises use of $m(F_o - F)$, where m is a slope of an $F-\omega$ characteristic, F_o is the power set point, and F is the measured power flow.

13. The method of claim 11, wherein calculating the operating frequency comprises use of $m(P_o - P)$, where m is a slope of a $P-\omega$ characteristic, P_o is the power set point, and P is the measured power flow.

14. The method of claim 12, wherein the measured power is the measured power flow.

15. The method of claim 11, wherein calculating the maximum frequency change comprises subtracting the measured power from the first power set point to determine a power differential.

16

16. The method of claim 15, wherein calculating the maximum frequency change further comprises applying the determined power differential to a proportional-integral controller.

17. The method of claim 11, wherein calculating the minimum frequency change comprises subtracting the measured power from the second power set point to determine a power differential.

18. The method of claim 17, wherein calculating the minimum frequency change further comprises applying the determined power differential to a proportional-integral controller.

19. The method of claim 11, further comprising regulating an output voltage of the generator using a voltage versus reactive power droop controller.

20. A microsource, the microsource comprising:
a generator;

a prime mover, the prime mover including a shaft connected to drive the generator to generate power at a frequency controlled by a rotation rate of the shaft; and

a controller operably coupled with the prime mover and the generator, the controller including circuitry

to calculate a maximum frequency change for the generator based on a first comparison between a first power set point and a measured power from the generator;

to calculate a minimum frequency change for the generator based on a second comparison between a second power set point and the measured power from the generator;

to calculate an operating frequency for the generator based on a third comparison between a power set point and a measured power flow;

to calculate a requested shaft speed for the prime mover by combining the calculated maximum frequency change, the calculated minimum frequency change, and the calculated operating frequency;

to calculate a shaft speed adjustment for the prime mover based on a fourth comparison between the calculated requested shaft speed and a measured shaft speed of the prime mover; and

to calculate a fuel command for the prime mover based on the calculated shaft speed adjustment to adjust the rotation rate of the shaft of the prime mover thereby controlling the frequency.

* * * * *